Plant Physiology Preview. Published on March 16, 2007, as DOI:10.1104/pp.106.091579

RUNNING HEAD: Role of MAM3 in Glucosinolate Formation

Jonathan Gershenzon

Hans-Knöll-Strasse 8

D-07745 Jena

GERMANY

Phone: +49-3641-57 1300

+49-3641-57 1301

Fax: +49-3641-57 1302

Email: gershenzon@ice.mpg.de

Category: Biochemical Processes and Macromolecular Structures

MAM3 Catalyzes the Formation of All Aliphatic Glucosinolate Chain Lengths in *Arabidopsis thaliana*

Susanne Textor,[a] Jan-Willem de Kraker,[a] Bettina Hause[b], Jonathan Gershenzon,[a,1] James G. Tokuhisa[a,2]

[a]Department of Biochemistry, Max Planck Institute for Chemical Ecology, Hans-Knöll Strasse 8, D-07745 Jena, Germany

[b]Department of Secondary Metabolism, Leibniz Institute of Plant Biochemistry, D-06018 Halle, Germany

The research was supported by the German National Science Foundation (grant GE 1126/1-3), the Max Planck Society and Virginia Polytechnic Institute.

[2]Current address: Department of Horticulture, Virginia Polytechnic Institute and State University, Blacksburg, VA 24061 USA

[1]To whom correspondence should be addressed: E-mail gershenzon@ice.mpg.de; fax 49-3641-571302

ABSTRACT

Chain elongated, methionine-derived glucosinolates are a major class of secondary metabolites in *Arabidopsis thaliana*. The key enzymatic step in determining the length of the chain is the condensation of acetyl-CoA with a series of ω-methylthio-2-oxoalkanoic acids, catalyzed by methylthioalkylmalate (MAM) synthases. The existence of two MAM synthases has been previously reported in the *A. thaliana* ecotype Columbia: MAM1 and MAM3 (formerly known as MAM-L). Here we describe the biochemical properties of the MAM3 enzyme which is able to catalyze all six condensation reactions of methionine chain elongation that occur in *A. thaliana*. Underlining its broad substrate specificity, MAM3 also accepts a range of non-methionine-derived 2-oxoacids, *e.g.* converting pyruvate to citramalate and 2-oxoisovalerate to isopropylmalate, a step in leucine biosynthesis. To investigate its role *in vivo*, we identified plant lines with mutations in *MAM3* that resulted in a complete lack or greatly reduced levels of long-chain glucosinolates. This phenotype could be complemented by reintroduction of a *MAM3* expression construct. Analysis of MAM3 mutants demonstrated that MAM3 catalyzes the formation of all glucosinolate chain lengths *in vivo* as well as *in vitro* making this enzyme the major generator of glucosinolate chain length diversity in the plant. The localization of MAM3 in the chloroplast suggest that this organelle is the site of methionine chain elongation.

INTRODUCTION

Plants synthesize an almost uncountable number of secondary metabolites. More than a 100,000 have been identified so far, which may represent only 10 % of the actual total in nature (Schwab, 2003; Wink, 2003). Only a small fraction of this diversity is present in individual plant species, yet single species contain multiple types of secondary metabolites and many representatives of a single type. For example, *Arabidopsis thaliana* is reported to produce over 170 secondary metabolites, including approximately 50 terpenes, 25 benzenoids and 20 phenylpropanoids (D'Auria and Gershenzon, 2005). In the last few years, researchers have begun to identify the biochemical bases of this diversity. In some cases, biosynthetic enzymes catalyze multiple product formation (Köllner et al., 2004; Tholl et al., 2005) or have broad substrate specificities (Wan and Wilkins, 1994; Gang et al., 2002). These properties may allow the generation of a large variety of secondary metabolites with a relatively small amount of biochemical machinery.

One of the largest groups of secondary metabolites in *A. thaliana* with 35 representatives is the glucosinolates (Reichelt et al., 2002) which serve as anti-herbivore defenses (Wittstock et al., 2003). These amino acid-derived compounds have variable side chains attached to a common core structure of a glucose residue linked via a sulfur atom to a (*Z*)-*N*-hydroximinosulfate ester (Fahey et al., 2001) (Fig. 1). The structural diversity of glucosinolates arises from different precursor amino acids, variation in side chain length and diverse patterns of secondary oxidation and esterification (Tokuhisa et al., 2004). The most abundant group of glucosinolates in *A. thaliana* consists of those derived from methionine. These are biosynthesized by the chain elongation of methionine followed by construction of the core glucosinolate skeleton and side chain modifications (Wittstock and Halkier, 2002; Halkier and Gershenzon, 2006).

Considerable attention has focused on chain elongation since it is a major contributor to the diversity of glucosinolate content and, as the first phase of glucosinolate biosynthesis, is responsible for the diversion of amino acid flux from primary to secondary metabolism. Glucosinolates of six different chain lengths are produced in *A. thaliana*. Studies with labeled methionine and acetate have shown that elongation of the methionine side chain involves a repetitive cycle of three reaction steps that result in the net addition of one methylene carbon for each turn of the cycle (Chisholm and Wetter, 1964; Lee and Serif, 1968, 1970; Graser et al., 2000). To enter the cycle, methionine is first deaminated to the corresponding 2-oxo-acid, 4-methylthio-2-oxobutanoic acid. An aminotransferase involved in this step has been

identified recently (Schuster et al., 2006). Elongation is initiated by condensation of the 2-oxo-acid with acetyl-CoA yielding a methylthioalkylmalate intermediate. Subsequently, isomerization and oxidation-decarboxylation reactions yield a 2-oxo acid that is extended by one methylene group. This product can undergo additional cycles of elongation or it can be transaminated to form an elongated amino acid which then enters the pathway for formation of the core glucosinolate structure. In the latter case, methionine elongated by a single methylene group would result in the formation of 3-methylthiopropylglucosinolate, referred to as a C_3 glucosinolate because of the three methylene groups in its side chain. C_4 to C_8 glucosinolates are the result of further chain elongations with C_8 representing the longest aliphatic glucosinolate type found in *A. thaliana*.

The chain-length spectrum of aliphatic glucosinolates in *A. thaliana* is critically influenced by whether the 2-oxo acid intermediates undergo further elongation or are diverted into glucosinolate core biosynthesis. Hence we have focused on the elongation cycle enzymes at this important branching point, the methylthioalkylmalate (MAM) synthases, which catalyze the condensation of 2-oxo acid derivatives of methionine with acetyl-CoA. The MAM synthases belong to a large family of enzymes that condense various 2-oxo acids with an acyl-CoA ester (Textor et al., 2004). One member of this group is isopropylmalate synthase (IPMS, EC 2.3.3.13), which condenses 2-oxo-isovalerate with acetyl-CoA, the chain elongation reaction in leucine biosynthesis.

Molecular studies on MAM synthases in *A. thaliana* began with the identification of four candidate genes in the Columbia accession (Col-0) that showed similarity to the IPMS-encoded genes of other organisms (Campos de Quiros et al., 2000; Kroymann et al., 2001). Two of these candidate genes are immediately adjacent to each other at the *GS-ELONG* locus on chromosome V (Magrath et al., 1994). Since this locus controls the dominant glucosinolate side chain length (C_3 or C_4), the genes were thought to encode MAM synthases. When heterologously expressed in *Escherichia coli*, one of these genes (At5g23010) was demonstrated to encode a protein that catalyzes the condensation reactions for two cycles of methionine chain elongation (Kroymann et al., 2001; Textor et al., 2004), and so was named *MAM1*. Plant lines with mutations in *MAM1* showed a decrease in C_4 glucosinolates and a corresponding increase in C_3 glucosinolates. However, the residual C_3 and C_4 glucosinolates in these lines, plus the continued accumulation of C_5-C_8 glucosinolates suggested the presence of additional MAM activities. Furthermore, MAM activity was detected in protein extracts of a mutant plant line (*gsm 1-1 = TU1*) lacking a functional *MAM1* allele (Textor et al., 2004).

The residual MAM activity may be ascribed to the product of the second gene at the *GS-ELONG* locus (At5g23020), named *MAM-L* for "MAM-like", since an insertion mutation in the *MAM-L* locus showed alterations in the biosynthesis of long-chain aliphatic glucosinolates (Field et al., 2004). It is not likely that this MAM activity arises from either of the other two candidate genes in *A. thaliana* with similarity to IPMS genes of other organisms. Both candidates, At1g74040 and At1g18500, have recently been shown to encode actual IPMSs by biochemical and molecular methods (de Kraker et al., 2006).

In this report, we describe an extensive biochemical characterization of the MAM-L enzyme showing that it does indeed account for the remaining MAM activity in *A. thaliana*. In addition to in vitro studies of the heterologously expressed enzymes with an extensive series of substrates, we determined the subcellular location of MAM-L and the relative steady-state levels of the transcript in various tissues. Furthermore, we determined glucosinolate content in mutant plant lines where the levels of MAM-L and MAM1 enzyme activity have been decreased through genetic alterations at the *MAM* loci. We propose that *MAM-L* be renamed *MAM3* based on the biochemical properties of the encoded enzyme demonstrated here, the existing rules for *A. thaliana* gene nomenclature, and the prior naming of *MAM1* and *MAM2* (Kroymann et al., 2003). To minimize confusion, Table 1 summarizes the disparate nomenclature used in previous publications for the five members of the methylthioalkylmalate / isopropylmalate synthase gene family in *A. thaliana*.

RESULTS

MAM3 Has Methylthioalkylmalate Synthase Activity

The open reading frame of the *MAM3* gene without the 5' sequence encoding a putative plastid targeting peptide was cloned from the Columbia accession into a plasmid construct containing the T7 viral promoter and a C-terminal polyhistidine peptide, and expressed in the *E. coli* BL21(DE3) strain. The recombinant protein was detected in the bacterial extract as a prominent band of the predicted size of 53 kDa by SDS-PAGE analysis. This extract exhibited methylthioalkylmalate synthase activity with 4-methylthio-2-oxobutanoic acid, the 2-oxo acid derived from methionine, and ^{14}C-labeled acetyl-CoA. Purification of the recombinant polyhistidine-containing protein by application to an Ni-NTA affinity chromatography resin and elution with L-histidine resulted in an active enzyme fraction that was more than 90% pure as judged by SDS-PAGE with Coomassie staining.

Basic characterization of MAM3 was performed by incubation with 4-methylthio-2-oxobutanoic acid and ^{14}C-labeled acetyl-CoA as substrates. The assay products were separated by radio-HPLC and the identity of the product, 2-(2'-methylthioethyl)-malate (MTEM), was confirmed by liquid chromatography-mass spectroscopy (LC-MS) in comparison with an authentic MTEM standard (Textor et al., 2004). The recombinant enzyme had a pH optimum at pH 8.0 with half maxima at pH 6.3 and 9.2 (range tested: pH 5.5-10 at intervals of 0.5). The temperature optimum was 32°C, with 70% activity at 25°C and 39°C (range tested: 22-40°C at intervals of 2°C). As in the case of MAM1 (Textor et al., 2004), MAM3 activity was dependent on the presence of a divalent cation with Mn^{2+} giving highest activity. If the MAM3 activity in the presence of Mn^{2+} is set to 100, then the addition of Fe^{2+} (59), Co^{2+} (41), Mg^{2+} (39) and Ca^{2+} (39) resulted in moderate activity, while that of Zn^{2+} (18), Mo^{2+} (17), Ni^{2+} (14) and Cu^{2+} (1) resulted in low activity. Consistent with this divalent cation dependency, product formation was inhibited 50% by 10 µM EDTA and completely by 40 µM EDTA. Unlike MAM1, the addition of ATP did not promote MAM3 activity; instead activity was reduced 50% by an ATP concentration of 18 mM. Similarly, there was no requirement for DTT, which was necessary at 1 mM for the activity of MAM1.

MAM3 Catalyzes All the Condensation Reactions of Glucosinolate Chain Elongation in *A. thaliana* in vitro, but with Different Efficiencies

To investigate the ability of MAM3 to catalyze the various condensation reactions of the chain elongation cycle of *A. thaliana* glucosinolate biosynthesis, the recombinant enzyme was incubated with a series of 2-oxo-acids of different chain lengths and substrate analogs where the sulfur atom is substituted with a methylene group. *A. thaliana* requires six different substrates for condensation reactions to produce the six different chain length glucosinolates (C_3-C_8) that it accumulates. The products of MAM3 activity were identified by LC-MS and confirmed in comparison to authentic standards (see Supplemental Fig. 1 online). The reactions catalyzed include all six condensations predicted to occur in *A. thaliana* using either the natural substrates or the non-sulfur analogs. The enzyme was unable to catalyze the reaction with the longest compound, 2-oxo-dodecanoic acid, the analog of the substrate leading to C_9 glucosinolates, which are not observed in *A. thaliana* (Table 2).

To compare the substrates, kinetic studies were done with the native substrates available (Table 3), all of which exhibited standard Michaelis-Menten kinetics. The K_m values obtained ranged from 932 µM for 4-methylthio-2-oxobutanoic acid to 81 µM for 9-methylthio-2-oxononanoic acid, suggesting increased substrate affinity with increasing chain

length. The k_{cat} values were highest with the medium chain length substrate (6-methylthio-2-oxohexanoic acid) and lower for the shorter substrates (4-methylthio-2-oxobutanoic acid and 5-methylthio-2-oxopentanoic acid) and the longer substrates (8-methylthio-2-oxooctanoic acid and 9-methylthio-2-oxononanoic acid). The resulting specificity constants (k_{cat}/K_m) for the substrate series reflect this trend also indicating that the intermediate chain length substrates are catalytically most efficient and the longest substrates are the least efficient. The K_m for acetyl-CoA was 2.3 mM and the k_{cat} value was 3.0 s^{-1}.

MAM3 Also Catalyzes Reactions with Other 2-Oxo Acids

Since the MAM3 enzyme has about 50% amino acid identity with *A. thaliana* proteins predicted to encode isopropylmalate synthases (which catalyze a step in leucine biosynthesis), it may also have this catalytic capability. The recombinant protein was tested with 2-oxoisovalerate (3-methyl-2-oxobutanoate), the substrate for the leucine biosynthetic reaction, and other 2-oxo acids. MAM3 was able to convert 2-oxoisovalerate (to isopropylmalate) and pyruvate (to citramalate), but based on their kinetic parameters, these were less preferred substrates than the methionine-derived 2-oxo acids involved in glucosinolate formation (Table 3). The enzyme also converted 4-methyl-2-oxopentanoate and 5-methyl-2-oxohexanoate to their malate-derivatives with specific acitvities of 422 ± 56 and 1070 ± 294 nmol min^{-1} mg^{-1}, respectively. These reactions represent the condensation reactions of a chain elongation cycle predicted for leucine-derived glucosinolates which have been identified in *A. thaliana* ecotypes (Kliebenstein et al., 2001; Reichelt et al., 2002). Additionally, the enzyme converted 3-methyl-2-oxopentanoate with a specific activity of 86 ± 9 nmol min^{-1} mg^{-1} to a product, representing the chain elongation reaction for isoleucine-derived glucosinolates, not yet described in *A. thaliana*. Finally, a reaction product was formed with phenylpyruvate (specific activity of 22 ± 4 nmol min^{-1} mg^{-1}), which represents the condensation reaction leading to phenylethylglucosinolate, a compound known from *A. thaliana* (Reichelt et al., 2002; Brown et al., 2003). A prior QTL mapping study that implicated the *GS-Elong* locus (which includes *MAM1, MAM2 and MAM3*) in controlling phenylalanine elongation for glucosinolate biosynthesis (Kliebenstein et al., 2001), supports the role of MAM3 in catalyzing reaction with phenylpyruvate in vivo.

To confirm the ability of MAM3 to catalyze isopropylmalate synthase activity *in vivo*, the auxotrophic *E. coli* strain CV512(DE3) which is lacking isopropylmalate synthase activity was transformed with vector constructs containing either the *E. coli leuA* gene (coding for the endogenous isopropylmalate synthase) or *MAM3* from *A. thaliana*. If MAM3 had

isopropylmalate synthase activity *in vivo*, it should complement the mutation by restoring the ability of CV512(DE3) to grow on a minimal medium without supplemental leucine. Under such conditions, growth was not observed with the negative control CV512(DE3), whereas the positive control, strain CV512(DE3) with the *leuA* construct, showed growth within 2 d when incubated at 37ºC, and within 3 d when incubated at 28ºC. No complementation was observed with the strain containing the *MAM3* construct when the cells were grown at 37ºC but colony growth was observed at 28ºC after 3 d of culture. Hence, the *A. thaliana MAM3* was able to complement the mutant in the gene encoding isopropylmalate synthase and restored autotrophic growth.

MAM3 is Targeted to the Chloroplasts

To learn more about subcellular localization of MAM3 an antibody was raised against the purified enzyme. The antibody was carefully tested for cross-reactivity with the other members of the MAM/IPMS family of *A. thaliana* (Columbia) and showed weak cross-reactivity only with MAM1 (Supplemental Fig.2). Immunolocalization experiments with leaf tissue of *A. thaliana* (Columbia) performed with the anti-MAM3 serum confirmed that MAM3 is targeted to the chloroplasts (Fig. 2) as predicted on the basis of its N-terminal sequence (Kroymann et al., 2001). Since the immediately preceding enzyme of the methionine chain elongation cycle, the aminotransferase, was recently shown to be localized in the cytosol (Schuster et al., 2006), this implies that the 2-oxo acid substrate of MAM3 is imported from the cytosol into chloroplasts.

MAM3* Mutants Lack Long-Chain Glucosinolates, and Their Production Can Be Restored by Ectopic Expression of *MAM3

To understand the role of MAM3 in determining the glucosinolate profile *in planta*, we characterized two mutant lines of the *A. thaliana* Columbia accession, one with a nucleotide alteration in the *MAM3* gene, and the other with a T-DNA insertion resulting in changes in *MAM3* gene expression.

The mutant line TU3 (*gsm2-1*) had been isolated and described briefly by Haughn et al. (Haughn et al., 1991) as lacking C_6, C_7 and C_8 aliphatic glucosinolates in the leaves. We confirmed these results in seeds, but found a minor amount of C_6 in leaves (Fig. 3). The absence of the longer aliphatic glucosinolates segregated as a recessive trait. Based on our biochemical characterization of MAM3, we considered it likely that the *gsm2-1* mutation was

in this gene. DNA sequence comparisons of wild-type and mutant *MAM3* clones revealed a base substitution in *gsm2-1* at position 788 relative to the predicted start of the open reading frame of the *MAM3*. The G to A transition, consistent with the alkylating activity of ethylmethanesulfonate used to generate the mutant population, results in a missense mutation converting a glycine to a glutamate codon.

To demonstrate that this mutation in *MAM3* was responsible for the altered glucosinolate profile, two different methods were used. First, the mutant enzyme G263E was created by site directed mutagenesis. When this enzyme was tested for MAM activity using the same conditions as for the wild type enzyme no activity could be found. Second, the *gsm2-1* mutant line was used for the transgenic expression of a gene construct consisting of the 35S promoter and the open reading frame of *MAM3*. Leaves from eight randomly selected individuals of a T_2 segregating population were analyzed for levels of the endogenous *MAM3* and *MAM1* transcripts, the introduced *MAM3* transcript and glucosinolate content. Three of these individuals (1-3, Table 4) had detectable levels of the introduced *MAM3* transcript and between 12-22 µmol per gram dry weight combined of C_6, C_7 and C_8 glucosinolates. These levels of long-chain, methionine-derived glucosinolates were about 5-fold higher than those detected in wild-type *A. thaliana* and demonstrate complementation of the *gsm2-1* mutant phenotype. In one individual, in which no transcript from the introduced *MAM3* gene was detectable by reverse transcriptase-PCR, there were also no detectable long-chained aliphatic glucosinolates (data not shown). The remaining four individuals exhibited 5-fold lower levels of the introduced transcript than those observed in the three complemented individuals, and showed aberrant sizes of endogenous *MAM1* and *MAM3* transcripts. These lines lacked long-chain, methionine-derived glucosinolates (data not shown) and had reduced (4-19 µmol per gram dry weight) levels of all aliphatic glucosinolates.

The Salk_007222 line (*gsm2-2*) is reported to contain a T-DNA insertion in the sixth intron of the *MAM3* gene. The report was confirmed by PCR using *gsm2-2* genomic DNA as a template with oligonucleotide primer pairs derived from the T-DNA insert and *MAM3* gene sequences (data not shown). The mutation generated a recessive phenotype consisting of a 90% reduction in C_8 glucosinolates in *gsm2-2* leaves relative to wild-type (Fig. 3). The seed of *gsm2-2* exhibited reductions in the levels of both C_7 and C_8 glucosinolates, although in both *gsm2-1* and *gsm2-2* the relative proportion of C_7 and C_8 to total glucosinolates was somewhat higher in the seeds than in the leaves.

MAM3 mutants lacked only long-chain glucosinolates even though *in vitro* the enzyme is capable of carrying out the condensation reactions necessary for forming the full range of

chain-lengths of methionine-derived glucosinolates occurring in *A. thaliana*. This apparent discrepancy is likely due to the presence of MAM1 (Kroymann et al., 2001; Textor et al., 2004). To learn more about MAM3 activity *in vivo*, we measured the glucosinolate profiles of a T-DNA insertion line (*gsm1-3*) in which the *MAM1* gene is disrupted. All glucosinolate chain lengths were evident with a large reduction in C_4 glucosinolates accompanied by a commensurate increase in C_3 glucosinolates as well as a slight increase in C_8 glucosinolates (Fig. 4). A very similar phenotype was described before for a *MAM*1 missense mutant (Haughn et al., 1991; Kroymann et al., 2001). To determine whether *MAM3* mutations affect non-aliphatic glucosinolates as well, we examined the correlations among the propyl, butyl and indolic classes. Across all *MAM3* mutants and the wild type, there was a positive correlation between propyl and indolic glucosinolates ($r = 0.84$, $P < 0.05$) and a negative correlation between butyl and indolic glucosinolates ($r = -0.88$, $P < 0.05$) indicating there might be metabolic crosstalk between the accumulation of aliphatic and indole glucosinolates.

The Organ Expression Profile of *MAM3* Transcripts is Different from That of *MAM1*

To identify the patterns of *MAM* gene expression in wild-type *A. thaliana* Columbia and the *MAM3* mutant lines, transcript levels for both *MAM1* and *MAM3* were determined relative to the transcript levels for the actin gene *ACT8* using reverse transcriptase-PCR on RNA extracted from root, leaf, flower and silique tissues.

In wild-type plants, the highest levels of expression of *MAM3* transcript were observed in the roots followed by the mature leaves, expanding leaves and siliques (Fig. 5). Under the cycle conditions used, transcript was not detected in stems (data not shown) and flowers. This profile differs from the pattern of *MAM1* transcript accumulation, where the highest levels were found in the expanding leaves followed by mature leaves, flowers, roots and siliques. The transcript profile for the *MAM3* mutant, *gsm2-1*, was similar to the wild-type profile as would be expected for a single base substitution mutation in the middle of an exon. For the *gsm2-2* line, with an insertion in *MAM3*, transcript levels for *MAM3* were lower than wild-type in all tissues. The reduction but not elimination of wild-type transcript levels is consistent with an insertion in the intron of *MAM3*, since it is likely that a low level of processing of the heteronuclear RNA occurs to remove the intron containing the T-DNA insert resulting in a detectable level of wild-type mRNA.

DISCUSSION

The aliphatic glucosinolates in *A. thaliana* are a large group of methionine-derived secondary metabolites (Halkier and Gershenzon, 2006). Their structural diversity arises in large part from the variable length of their side chains. Chain elongation of methionine proceeds by a repetitive three-step cycle in which the first step, the condensation of a 2-oxo acid with acetyl-CoA (Fig.1), is catalyzed by enzymes known as methylthioalkylmalate (MAM) synthases (Kroymann et al., 2001; Falk et al., 2004; Textor et al., 2004; Benderoth et al., 2006). Based on mutant analyses it was recently suggested that MAM3 (MAM-L) catalyzes the condensation reactions leading to long-chain glucosinolates (Field et al., 2004). However, in this study we demonstrate that MAM3 actually carries out all six condensation reactions leading to chain elongation *in planta*, and thus shapes the complete aliphatic glucosinolate profile of *A. thaliana*.

MAM3 Has a Very Broad Substrate Specificity for 2-Oxo Acids

The enzymatic properties of MAM3 heterologously expressed in *E. coli* were generally similar to those previously described for the *A. thaliana* MAM1 (Textor et al., 2004) and the MAM enzymes from other species like *Eruca sativa* (Falk et al., 2004), *Arabidopsis lyrata* and *Boechera stricta* (Benderoth et al., 2006) in the pH and temperature optima and the requirement for a divalent cation. However, in contrast to MAM1, MAM3 was not activated by ATP, had no dithiothreitol requirement, and had a K_m for acetyl-CoA (2.3 mM) that was nearly 10-fold higher than that of MAM1 (245 μM) and the *E. sativa* enzyme (340 μM). In comparing the amino acid sequences of MAM3 and MAM1 (the gene encoding the *E. sativa* enzyme has not yet been isolated), no ATP binding site motifs are apparent that might explain the different effects of this nucleotide. However, there are differences between MAM3 and MAM1 in the number (11 vs. 9) of cysteine residues that might result in differences in the number of disulfide bridges present in the enzyme and thus in its dithiothreitol requirement. Currently nothing is known about the secondary and tertiary structure of the MAM enzymes. The crystal structure of a distantly related protein, the IPMS of *Mycobacterium tuberculosis*, does not have any disulfide bridges and the enzyme shows no requirement for dithiothreitol for activity (Koon et al., 2004, 2004).

The most striking difference between MAM3 and other MAM enzymes studied to date is the much broader substrate specificity of MAM3. This enzyme accepts all six of the ω-methylthio-2-oxo acids employed in aliphatic glucosinolate chain elongation reactions in *A. thaliana*. MAM1 uses only the three shortest of this series, 4-methylthio-2-oxobutanoate, 5-

methylthio-2-oxopentanoate and, at low levels, 6-methylthio-2-oxohexanoate (Textor et al., 2004; Benderoth et al., 2006). MAM2 from the *A. thaliana* accession *Landsberg erecta*, the *E. sativa* MAM and the MAMs of other species investigated so far are even more specialized and use only the very shortest ω-methylthio-2-oxo acid, 4-methylthio-2-oxobutanoate, as a substrate (Falk et al., 2004; Benderoth et al., 2006). MAM3 also accepts a variety of other 2-oxo acid substrates showing substantial activity with pyruvate and 2-oxoisovalerate, with k_{cat} values in the same range as for the substrates involved in methionine chain elongation. Though these characteristics were determined for a recombinant protein lacking the plastid targeting sequence and expressed heterologously in *E. coli*, they are likely to be representative of the characteristics of the native protein. Previous results show that the properties of recombinant MAM1 expressed in an analogous manner corresponded very closely to those of the native MAM protein purified from *A. thaliana* (Textor et al., 2004).

In vitro MAM3 converts pyruvate to citramalate, a metabolite previously identified in *A. thaliana* (Fiehn et al., 2000), and so this reaction may be catalyzed by MAM3 *in planta* as well. MAM3 also converts 2-oxoisovalerate to isopropylmalate, an important branch-point reaction of leucine biosynthesis. The isopropylmalate synthase (IPMS) activity of MAM3 is not surprising given that this protein shares over 50% sequence identity at the amino acid level to the products of the two genes shown to serve as IPMSs in this species (Kroymann et al., 2001; Field et al., 2004; de Kraker et al., 2006). However, it is not clear if MAM3 participates in leucine biosynthesis *in planta*. Previous work showed that MAM3 expression could complement an *E. coli* mutant (*LeuA*) lacking IPMS (Junk and Mourad, 2002). However, Field et al. (Field et al., 2004) failed to observe this complementation. In the light of these contradictory results, we repeated the experiment and did observe functional complementation in the presence of the *MAM3* when expression was done at 28 °C, but not at 37 °C. These results, together with the chloroplast localization of MAM3, provide support for the ability of this enzyme to catalyze condensation with 2-oxoisovalerate *in vivo*. Isopropylmalate synthase activity in spinach is reported to be localized in chloroplasts (Hagelstein and Schultz, 1993). However, since the specific activity of the IPMSs for 2-oxoisovalerate is at least 40 times higher than those of MAM3 it appears very unlikely that this enzymes is active as IPMS under normal growth conditions (de Kraker et al., 2006). Final proof of whether or not MAM3 can function in leucine formation in *A. thaliana* requires further investigations with lines carrying mutations in both *IPMS* genes.

MAM3 Catalyzes the Formation of All Glucosinolate Chain Lengths *in Vivo* as Well as *in Vitro*

Our investigations of *A. thaliana* lines with altered *MAM3* or *MAM1* expression levels demonstrated that the broad specificity of the MAM3 enzyme *in vitro* is also realized *in vivo*. Given that the only two other MAM-like proteins in *A. thaliana* (ecotype Columbia), the IPMSs, are highly unlikely to carry out a MAM reaction *in vivo* (de Kraker et al., 2006), the best measure of the catalytic abilities of MAM3 *in vivo* is the glucosinolate profile of the *MAM1* insertion mutant, *gsm1-3* (Fig. 4). Although a low level of *MAM1* transcript is detectable in this mutant (see Supplemental Fig. 3 online), the near identity of the glucosinolate phenotype with the previously described *MAM1* mis-sense mutant (Kroymann et al., 2001) suggests that it is a virtual knock-out. According to the glucosinolate profile of *gsm1-3*, MAM3 activity results in a leaf glucosinolate profile of all chain lengths C_3-C_8 dominated by C_3 and C_8.

The scope of MAM1 catalytic activity *in vivo*, on the other hand, should be observed mostly clearly in the *MAM3* knock-out mutants. We found that the T-DNA insertion line (*gsm2-2*) had reduced C_7 and C_8 glucosinolates, a finding also reported previously for another insertion line of this gene, which additionally lacked C_6 (Field et al., 2004). Consistent with these results, a line (*gsm2-1*) with a missense mutation in *MAM3* lacked any long chain glucosinolates and this phenotype was complemented by ectopic expression of *MAM3*. The short chain-length glucosinolates that are still present in these *MAM3* mutants (with C_4 being dominant just as in wild type) must therefore be produced by MAM1.

The wild type glucosinolate profile is clearly the result of the interplay of the two MAM enzymes, with MAM3 creating the basic profile consisting of all chain lengths from C_3 to C_8, but dominated by C_3 and C_8 glucosinolates. In wild type plants, this profile becomes modified by the actions of MAM1, which inverts the C_3/C_4 ratio and thus makes C_4 glucosinolates the most dominant type in *A. thaliana* Columbia. It is noteworthy that a QTL mapping approach to discovering the locus responsible for changing the C_3/C_4 ratio first identified the location of MAM1 (Magrath et al., 1994; Campos de Quiros et al., 2000; Kroymann et al., 2001). Final proof of the *in vivo* roles of MAM1 and MAM3 would be facilitated by analysis of a line mutated in both of these genes. Unfortunately, we failed to obtain such a double mutant either from crosses between lines carrying the single mutations or from attempts to co-suppress both genes.

MAM3 is a Major Generator of Glucosinolate Structural Diversity

The structural diversity of aliphatic glucosinolates in *A. thaliana* is due in large part to the variety of chain lengths present as well as the different types of secondary modifications that occur to the side chain (Halkier and Gershenzon, 2006). The variety of chain lengths formed is a direct consequence of the nature of the elongation process in which additional methylene groups are added one at a time to the parent methionine skeleton in a cyclic process so that intermediates of all chain lengths in the series C_3-C_8 are made. The broad substrate specificity of MAM3, which catalyzes the chain elongation reaction of the elongation cycle, is what facilitates this stepwise elongation process and so makes the variety possible.

Broad substrate specificity is a hallmark of many enzymes of secondary metabolism and contributes to the enormous diversity of this class (*e.g.*, (Gang et al., 2002)). For example, many enzymes of the core glucosinolate biosynthetic pathway have broad tolerance for various aliphatic, aromatic and indole side chains (Halkier and Gershenzon, 2006; Piotrowski et al., 2004), although the CYP79 (Chen et al., 2003; Mikkelsen et al., 2003) and CYP83 (Naur et al., 2003) series are more class specific. This allows many different types of glucosinolates to be made with the same set of enzymes. Similar low substrate specificities are known for enzymes of alkaloid and phenylpropanoid formation (Frick and Kutchan, 1999; Gang et al., 2002). Our knowledge of the enzymology of secondary metabolism is beginning to shed light on the biochemical bases of the enormous structural diversity observed. The next challenge will be to explain the functional significance of such diversity in the life of the plant.

MATERIALS AND METHODS

Chemicals and Plant Lines

Unless specified all chemical reagents including enzyme substrates and authentic standards for reaction products were obtained from Aldrich, Fluka, Merck, or Sigma. For the enzyme assays, [1-^{14}C]acetyl-CoA was purchased from Amersham Biosciences or Hartmann (Braunschweig, Germany). The following chemicals were custom synthesized as indicated: 5-methylthio-2-oxopentanoic acid, 6-methylthio-2-oxohexanoic acid and 9-methylthio-2-oxononanoic acid (Applichem GmbH, Darmstadt, Germany); 8-methylthio-2-oxooctanoic acid (Hochschule Zittau/Görlitz, Germany). Synthesis of 2-oxoheptanoic acid was described previously (Falk et al., 2004). 2-Oxononanoic acid, 2-oxodecanoic acid, 2-oxoundecanoic

acid, 2-oxododecanoic acid and 5-methyl-2-oxohexanoic acid were synthesized by a Claisen condensation between diethyl oxalate and the respective aliphatic (C_{n-1}) ethyl ester, yielding a diethyl 2-alkyl-3-oxosuccinate product that was subsequently hydrolyzed and decarboxylated under reflux with hydrochloric acid (Schreiber, 1956; Nakamura et al., 1988). Experimental conditions were essentially the same as described for the synthesis of 2-oxo-heptanoic acid (Falk et al., 2004), except that the 2-oxo acid product was not isolated from the residual oil by vacuum distillation but by crystallization with potassium carbonate (Roxburgh, 1997). Hence, the reaction mixture resulting from refluxing with HCl was three times extracted with diethyl ether (3 × 50 mL) and the combined layers were dried with sodium sulfate. After removal of the solvent under reduced pressure, the residual oil was redissolved in twice its volume of diethyl ether and potassium carbonate was added slowly up to the point where no more gas bubbles were released. The supernatant was decanted and the crystals formed rinsed with ether over a Büchner funnel. The crystals were suspended in 50 mL of diethyl ether and 1 M of HCl was added slowly to accommodate gas release up to pH 3. After shaking, the ether layer was separated, dried with sodium sulfate, and evaporated to yield the pure 2-oxo acid. The products were verified by mass spectroscopy and NMR. Overall yields were 9-12 %.

Authentic standards for the reaction products, hexylmalate and nonanylmalate were synthesized from methylheptanoate and methyldecanoate respectively, using essentially the 3-step procedure previously described (Chapple et al., 1988) for the synthesis of 2-methylthioethylmalate. However, hydrolysis of the nitrile groups to yield the carboxylic groups present in the alkylmalate products was done under more severe conditions by boiling in 66% sulfuric acid under reflux for 2 hours (Vogel and Furniss, 1996). The 80 mL reaction mixture was then poured into 100 mL of crushed ice and extracted with ethyl acetate (3 × 70 mL). The ethyl acetate layers were combined and the solvent removed under reduced pressure. The brown residue was dissolved in 70 mL diethyl ether and extracted with 5% aqueous sodium carbonate (3 × 50 mL). The aqueous layers were combined, acidified and extracted with diethyl ether (3 × 50 mL). The combined ether layers were dried and after removal of the solvent, and the residue was crystallized in chloroform-hexane (2:1) yielding the pure alkylmalate product in 6-7 % overall yield. The products were verified by mass spectroscopy and NMR.

The *A. thaliana* lines used in this study were obtained from the Arabidopsis Biological Resource Center and include (stock number): Columbia (CS3879), *gsm1-3* (S057539), *gsm2-1* (= TU3, CS2228) and *gsm2-2* (S007222).

RNA Extraction, Preparation for RT-PCR and *MAM3* Cloning

Total RNA was isolated from all tissues but siliques with Trizol (Invitrogen) according to the manufacturer's instructions. Total RNA was extracted from siliques using a hot borate procedure modified from Wan and Wilkins (Wan and Wilkins, 1994).

Reverse transcriptase reactions were done with MMLV-reverse transcriptase (Promega) using the reagents and instructions provided. In brief, 2 µg of total RNA was incubated with 0.5 µg of specific or dT_{12-18} oligonucleotide primers (Invitrogen) at 65°C for 5 min and cooled to 4°C. Enzyme reaction buffer and 200U of MMLV-reverse transcriptase were added to the RNA-primer mix and allowed to incubate at 42°C for 1 hr. The reaction mix was heated to 70°C for 10 min and stored at -80°C until use.

To isolate the MAM3 open reading frame, a cDNA preparation was generated by a reverse transcriptase reaction with RNA extracted from roots of the Columbia wild-type accession and primed with 2MAMLb (see Supplemental Table 1 online). In addition, a total DNA extract of a 1-2 kb size-selected cDNA phage library prepared from Columbia leaf RNA (by J. Shockey, Washington State University) was screened by PCR using Pfu DNA polymerase (Stratagene). Products were obtained using the oligonucleotide primers, 1MAMLa and 2MAMLb (see Supplemental Table 1 online), which include the start and stop codons, respectively, of the gene predicted at AGI locus At5g23020. Both preparations yielded identical *MAM3* ORFs.

To prepare *MAM3* for heterologous expression in bacteria, a putative chloroplast transit peptide and cleavage site were identified in the deduced amino acid sequence of *MAM3* by a neural network search algorithm (Emanuelsson et al., 2000) (http://www.cbs.dtu.dk/services/ChloroP/). The oligonucleotide primers 1MAM3h and 2MAM3k (see Supplemental Table 1 online) were designed to generate a truncated clone of the open reading frame of MAM3 lacking the predicted transit peptide sequence of 51 amino acids. This product was cloned into the pBAD-vector (Invitrogen). However, only a limited amount of protein was obtained after induced expression. Thus, *MAM3* was amplified by PCR from the pBAD construct with the primers MAMLex1ff and MAMLex1rv (see Supplemental Table 1 online). The resulting 1359 bp fragment was cloned into the pCRT7/CT-Topo vector (Invitrogen, Netherlands) using the pCR®T7 Topo TA cloning® kit (Invitrogen, Netherlands). The resulting MAM3 gene construct lacked the first 153 nucleotides of the ORF corresponding to the predicted transit peptide at the N-teminus and included nucleotide sequence coding for a hexahistidine peptide at the C-terminus.

Overexpression, Protein Purification, Antibody Production and Site Directed Mutagenesis

E. coli strain BL21(DE3) (Studier et al., 1990) containing the *MAM3* construct was grown at 37ºC on LB medium (Invitrogen) in the presence of ampicillin (100 µg/mL) to an optical density at 600 nm of 0.6, induced with 1 mM isopropyl-ß-D-thiogalactoside (IPTG) for 2 h and harvested. Cells were resuspended in buffer (50 mM Tris, pH 8.0, 1 mM $MgCl_2$) and disrupted by sonication (Bandelin Sonoplus HD2070, Berlin). The extract was clarified by centrifugation (6500 x g, 10 min) and the supernatant mixed with Ni-NTA agarose (Qiagen, Germany). Enzyme purification was carried out in a batch procedure. After two washing steps (sonication buffer, sonication buffer with 50 mM L-histidine), MAM3 was eluted from the resin with 50 mM Tris, pH 8.0, buffer containing 1 mM $MgCl_2$ and 200 mM L-histidine. Neither the presence of L-histidine (3-30 mM in the final assay depending on dilution) nor possible Ni^{2+}-leakage from the Ni-NTA agarose column had any influence on MAM3 activity as determined by comparison of a portion of direct NTA eluate to a fully-desalted eluate redissolved in 50 mM Tris, pH 8.0. Hence the NTA eluate was used directly for characterization. When investigating ion dependency (including the experiments with EDTA) and determining kinetic parameters, MAM3 was purified without Mg^{2+} in the buffers and still retained partial activity which could be fully restored with cation addition. Although our previous work with MAM1 and a MAM3-containing fraction showed these to be monomers (Textor et al., 2004), the recombinant enzyme was present in a partially dimeric form based on analysis by gel-filtration, probably due to the poly-histidine tag. However, there was no difference in substrate specificity between the two forms.

For antibody production, MAM3 purified as described above was subjected to gel-filtration on Superdex 200 (Amersham). MAM3 eluted as a dimer and was used to raise antibodies in rabbits. The anti-MAM3 antibody was purified from the crude antiserum by affinity chromatography with MAM3 coupled to a matrix (Davids Biotechnology, Regensburg)

Site directed mutagenesis of MAM3 was performed with the QuikChange® Site-Directed Mutagenesis Kit (Stratagene) using the primer pair Mut5ff/rv (see Supplemental Table 1 online).

Condensation Reaction Enzyme Assay

The enzyme assay for the condensation reaction between acetyl-CoA and 2-oxo-acids was carried out in general as previously described (Kroymann et al., 2001). The standard assay contained 100 mM Tris, pH 8.0, 4 mM $MnCl_2$, 1 mM acetyl-CoA, 9-17 µM [1-^{14}C]acetyl-CoA (50 µCi/mL, 47 mCi/mmol), 3 mM of the 2-oxoacid, and 10-20 µg of Ni-NTA agarose-purified enzyme in a total volume of 250 µL. Despite the variation in chain length, all substrates dissolved completely in the assay buffer. For enzyme kinetics the assay was incubated at 32ºC, the optimal temperature of the enzyme, and stopped by the addition of 750 µL ethanol.

Assay products except for those from long chain 2-oxoacid substrates were analyzed by ion exclusion HPLC (Nucleogel ion-300 OA, Macherey and Nagel, Düren, Germany) and detected by a flow-through radioactivity monitor (Radiomatic 500TR, Packard, Dreieich, Germany) as described (Kroymann et al., 2001). Assays with long 2-oxo acid substrates (8-methylthio-2-oxooctanoic acid, 9-methylthio-2-oxononanoic acid, 2-oxononanoic acid and its longer derivatives) were additionally analyzed on a reverse phase column (Supelcosil^{TM}LC-18-DB, Supelco, 25 cm x 2.1 mm, 5 µm) eluted with a mixture of 0.1% formic acid (solvent A) and acetonitrile (solvent B) at 0.25 mL/min with the following program: 0 min 20% B, 25 min 70% B, 26 min 100% B, total run time 37 min.

The general enzymatic properties of MAM3 and kinetic data for acetyl-CoA were determined over a range of 0.05 – 4 mM with 2-oxo-4-methylthiobutanoic acid as the cosubstrate at a 3 mM concentration. The assays for kinetic analysis of the 2-oxo acid substrates all contained 1 mM acetyl-CoA and a variable concentration of the 2-oxo acid ranging from 0.2 - 300 % of the determined K_m value. Divalent cations were tested with either Cl^- or SO_4^{2-} as counter-ions by direct addition to the enzyme assay in 4 mM concentration. All assays were conducted in the linear range with respect to time and protein concentration and were repeated at least five times per substrate. Protein was quantified according to the method of Bradford using bovine serum albumin as a standard. Michaelis-Menten kinetic parameters were determined using the EKI3 software program (Tuebingen University) which uses a nonlinear regression method described by Wilkinson (Wilkinson, 1961).

Bacterial Complementation

E. coli CV512 (F^+ leuA371, (Somers et al., 1990)) which is deficient in isopropylmalate synthase, was used for complementation studies. This strain is able to grow on M9-minimal medium with glucose as the carbon source when supplemented with Casaminoacids (Difco) or

transformed with a construct containing a functional isopropylmalate synthase. To ensure expression of T7-polymerase driven constructs, the IPTG inducible T7-polymerase gene was introduced into strain CV512 by the λDE3 lysogenisation kit (Novagen) giving CV512(DE3). A pET28a (Novagen) construct containing the *E. coli* DH5α (Hanahan, 1983) isopropylmalate synthase gene *leuA* was used for complementation studies as a positive control. The *leuA* gene was amplified by PCR from genomic DNA of DH5*a* with the primer pair IPMEff/IPMErv (see Supplemental Table 1 online) and cloned into pET28a using the *BamHI*/*XhoI* restriction sites provided by the primers. Complementation efficiency was tested at two different incubation temperatures, 28ºC and 37ºC.

Immunocytochemistry

Freshly harvested rosette leaves of *A. thaliana* ecotype Columbia were fixed in phosphate buffered saline (PBS; 135 mM NaCl, 3 mM KCl, 1.5 mM KH_2PO_4, 8 mM Na_2HPO_4) containing 4% (w/v) paraformaldehyde and 0.1% (v/v) Triton X-100, embedded in polyethylene glycol and cut as described by Hause et al. (Hause et al., 1996). Sections of 2-µm thickness were labelled with the rabbit anti-MAM3 antibody diluted 1:500 in PBS containing 1 % (w/v) acetylated BSA and 4.5 % (w/v) BSA. Subsequently, an anti-rabbit-IgG antibody conjugated with AlexaFluor 488 (Molecular Probes, Leiden, The Netherlands) was used according to the supplier's instructions. Standard washes followed each antibody incubation. Sections were counterstained with 0.1 $\mu g \cdot mL^{-1}$ 4,6-diamidino-2-phenylindole (DAPI; Sigma) and analysed using an Axioscop2 (Carl Zeiss, Jena, Germany) equipped with the proper filter combinations. Micrographs were taken with a CCD camera (Sony, Japan) and were processed through the Photoshop 8.0.1 program (Adobe).

Extraction of Genomic DNA

Genomic DNA was extracted from expanding leaves using the abbreviated protocol of Rogers and Bendich (Rogers and Bendich, 1985). About 5 mg of young leaf tissue was collected in a 1.5 mL microfuge tube and homogenized with 10 µL of 2x-CTAB Solution (2% cetyltrimethylammonium bromide (w/v), 100 mM Tris, pH 8.0, 20 mM EDTA, 1.4 M NaCl, 1.0% polyvinylpyrrolidone of 40,000 MW) using a micropestle. The sample was incubated at 65 ^{o}C for 1-2 min., cooled briefly on ice, and extracted with 10 µL of chloroform/isoamyl alcohol (24:1). Then, about 5-10 µL of H_2O was added, and the samples were centrifuged at 11,000*g*. The upper phase was recovered and 0.1 to 0.5 µL was used per 20-100 µL PCR.

Reverse Transcriptase PCR

cDNAs for *ACT8*, *MAM1* and *MAM3* were generated by reverse transcriptase (RT) reactions of 2 µg of RNA with dT_{12-18} oligonucleotide primers. For each PCR reaction, 20 µL solutions were prepared consisting of 1x PCR buffer (Promega, Madison), 0.2 mM dNTP, 0.5 µM each primer (see Supplemental Table 1 online for specific primer pairs), 16 ng of template RNA, and 0.7 U of Taq Polymerase (Promega). The reactions were subjected to an initial thermal denaturation of 94°C for 2 min, followed by 28 cycles at 94°C for 30 s, 53°C for 30 s and 72°C for 30 s, and ending with an incubation at 72°C for 2 min. Amplicon formation was determined to be linear for these reaction conditions. Reaction products were fractionated along with DNA standards (Low Mass Ladder, Invitrogen) by electrophoresis on 1% agarose gels and visualized by UV fluorescence after incubation of gels in 0.5 µg/mL ethidium bromide for 15 min. Band fluorescence was normalized with a gel documentation system (GeneGenius, Synoptics, Cambridge, UK) against *ACT8* product (GeneTools Analysis Software Version 3.02, Synoptics). PCRs for each RT reaction and oligonucleotide primer pair were done at least four times and each RT reaction was done in duplicate.

Cloning of *MAM3* for Plant Expression and Transformation

The ORF of the *MAM3* gene was cloned into pCR-Blunt II-TOPO (Invitrogen). A clone was identified that had wild-type sequence and was oriented such that the *XhoI* restriction site was at the 5'-end and the *KpnI* restriction site was at the 3'-end of the ORF. The ORF was cloned into the primary pART7 vector (Gleave, 1992) at the *XhoI* and *KpnI* sites between the 35S promoter of cauliflower mosaic virus and the octopine synthase transcriptional terminator. The expression construct was excised and transferred to the binary vector pART27 (Gleave, 1992). The *Agrobacterium tumefaciens* strain GV3101 was transformed with the plasmid using spectinomycin as the selectable marker (Holsters et al., 1978). *A. thaliana* plants were inoculated with the transformed *A. tumefaciens* using a modification of the vacuum infiltration method of Bechtoldt et al. (Bechtold et al., 1993).

Glucosinolate Extraction, Identification and Quantification

Glucosinolate extraction and purification were done as previously described (Brown et al., 2003). The desulfoglucosinolate fractions were separated by HPLC on an Agilent HP1100

System using a C-18, fully end-capped, reverse phase column (LiChrospher RP-18, 250x4.6 mm i.d., 5 µM particle size, Chrompack). Procedures for the identification and quantification of individual desulfoglucosinolates were described previously (Brown et al., 2003).

Accession Numbers

Sequence data from this article can be found in the EMBL/GenBank data libraries under accession numbers At1g49240 (*AC8*), At5g23010 (*MAM1*), At5g23020 (*MAM3*, former *MAM-L*), At1g18500 (*IPMS1*) and At1g74040 (*IPMS2*).

Supplemental Material

The following materials are available in the online version of this article.

Supplemental Figure 1. Chromatograms and mass spectrometry data of MAM3 reaction products.

Supplemental Figure 2. Western Blot showing the specificity of anti-MAM3.

Supplemental Figure 3. Semi-quantitative RT-PCR of steady-state transcript levels for genes *AC8*, *MAM1* and *MAM3* in the leaves of wild-type Columbia (wt) and the mutant line *gsm1-3*.

Supplemental Table 1. Oligonucleotide primers used in this study.

ACKNOWLEDGEMENTS

We thank Nadine Gerth and Katrin Luck for technical assistance, Stefan Bartram for advice on substrate synthesis, and Ales Svatos for mass spectrometry of the reaction products.

LITERATUR CITED

Bechtold N, Ellis J, Pelletier G (1993) In-planta Agrobacterium mediated gene transfer by infiltration of adult Arabidopsis thaliana plants. C.R.Acad.Sci.[III]. **316:** 1194-1199

Benderoth M, Textor S, Windsor AJ, Mitchell-Olds T, Gershenzon J, Kroymann J (2006) Positive selection driving diversification in plant secondary metabolism. Proc Natl Acad Sci U S A **103:** 9118-9123

Brown PD, Tokuhisa JG, Reichelt M, Gershenzon J (2003) Variation of glucosinolate accumulation among different organs and developmental stages of Arabidopsis thaliana. Phytochemistry **62:** 471-481

Campos de Quiros H, Magrath R, McCallum D, Kroymann J, Schnabelrauch D, Mitchell-Olds T, Richard M (2000) α-Keto acid elongation and glucosinolate biosynthesis in Arabidopsis thaliana. Theor Appl Genet **101:** 429-437

Chapple CCS, Decicco C, Ellis BE (1988) Biosynthesis of 2-(2'-methylthio)ethylmalate in Brassica carinata. Phytochemistry **27:** 3461-3463

Chen S, Glawischnig E, Jorgensen K, Naur P, Jorgensen B, Olsen CE, Hansen CH, Rasmussen H, Pickett JA, Halkier BA (2003) CYP79F1 and CYP79F2 have distinct functions in the biosynthesis of aliphatic glucosinolates in Arabidopsis. Plant J **33:** 923-937

Chisholm MD, Wetter LR (1964) Biosynthesis of mustard oil glucosides: IV. The administration of methionine-C^{14} and related compounds to horseradish. Canadian Journal of Biochemistry **42:** 1033-1040

D'Auria JC, Gershenzon J (2005) The secondary metabolism of Arabidopsis thaliana: growing like a weed. Curr Opin Plant Biol **8:** 308-316

de Kraker JW, Luck K, Textor S, Tokuhisa JG, Gershenzon J (2006) Two Arabidopsis Genes (IPMS1 and IPMS2) Encode Isopropylmalate Synthase, the Branchpoint Step in the Biosynthesis of Leucine. Plant Physiol **143:** 970-986

Emanuelsson O, Nielsen H, Brunak S, Von Heijne G (2000) Predicting subcellular localization of proteins based on their N-terminal amino acid sequence. J Mol Biol **300:** 1005-1016

Fahey JW, Zalcmann AT, Talalay P (2001) The chemical diversity and distribution of glucosinolates and isothiocyanates among plants. Phytochemistry **56:** 5-51

Falk KL, Vogel C, Textor S, Bartram S, Hick A, Pickett JA, Gershenzon J (2004) Glucosinolate biosynthesis: Demonstration and characterization of the condensing enzyme of the chain elongation cycle in Eruca sativa. Phytochemistry **65:** 1073-1084

Fiehn O, Kopka J, Dormann P, Altmann T, Trethewey RN, Willmitzer L (2000) Metabolite profiling for plant functional genomics. Nat Biotechnol **18:** 1157-1161

Field B, Cardon G, Traka M, Botterman J, Vancanneyt G, Mithen R (2004) Glucosinolate and amino acid biosynthesis in Arabidopsis. Plant Physiol **135:** 828-839

Frick S, Kutchan TM (1999) Molecular cloning and functional expression of O-methyltransferases common to isoquinoline alkaloid and phenylpropanoid biosynthesis. Plant J **17:** 329-339

Gang DR, Beuerle T, Ullmann P, Werck-Reichhart D, Pichersky E (2002) Differential production of meta hydroxylated phenylpropanoids in sweet basil peltate glandular trichomes and leaves is controlled by the activities of specific acyltransferases and hydroxylases. Plant Physiol **130:** 1536-1544

Gleave AP (1992) A versatile binary vector system with a T-DNA organisational structure conducive to efficient integration of cloned DNA into the plant genome. Plant Mol Biol **20:** 1203-1207

Graser G, Schneider B, Oldham NJ, Gershenzon J (2000) The methionine chain elongation pathway in the biosynthesis of glucosinolates in Eruca sativa (Brassicaceae). Arch Biochem Biophys **378:** 411-419

Hagelstein P, Schultz G (1993) Leucine synthesis in spinach chloroplasts: partial characterization of 2-isopropylmalate synthase. Biological Chemistry Hoppe-Seyler **374:** 1105-1108

Halkier BA, Gershenzon J (2006) Biology and biochemistry of glucosinolates. Annu Rev Plant Biol **57:** 303-333

Hanahan D (1983) Studies on transformation of Escherichia coli with plasmids. J Mol Biol **166:** 557-580

Haughn GW, Davin L, Giblin M, Underhill EW (1991) Biochemical genetics of plant secondary metabolites in Arabidopsis thaliana - the glucosinolates. Plant Physiol **97:** 217-226

Hause B, Demus U, Teichmann C, Parthier B, Wasternack C (1996) Developmental and tissue-specific expression of JIP-23, a jasmonate-inducible protein of barley. Plant Cell Physiol **37:** 641-649

Holsters M, de Waele D, Depicker A, Messens E, Van Montagu M, Schell J (1978) Transfection and transformation of Agrobacterium tumefaciens. Mol Gen Genet **163:** 181-187

Junk DJ, Mourad GS (2002) Isolation and expression analysis of the isopropylmalate synthase gene family of Arabidopsis thaliana. J Exp Bot **53:** 2452-2454

Kliebenstein DJ, Gershenzon J, Mitchell-Olds T (2001) Comparative quantitative trait loci mapping of aliphatic, indolic and benzylic glucosinolate production in *Arabidopsis thaliana* leaves and seeds. Genetics **159:** 359-370

Kliebenstein DJ, Lambrix VM, Reichelt M, Gershenzon J, Mitchell-Olds T (2001) Gene duplication in the diversification of secondary metabolism: Tandem 2-oxoglutarate-dependent dioxygenases control glucosinolate biosynthesis in Arabidopsis. Plant Cell **13:** 681-693

Köllner TG, Schnee C, Gershenzon J, Degenhardt J (2004) The variability of sesquiterpenes emitted from two Zea mays cultivars is controlled by allelic variation of two terpene synthase genes encoding stereoselective multiple product enzymes. Plant Cell **16:** 1115-1131

Koon N, Squire CJ, Baker EN (2004) Crystal structure of LeuA from Mycobacterium tuberculosis, a key enzyme in leucine biosynthesis. Proc Natl Acad Sci U S A **101:** 8295-8300

Koon N, Squire CJ, Baker EN (2004) Crystallization and preliminary X-ray analysis of alpha-isopropylmalate synthase from Mycobacterium tuberculosis. Acta Crystallogr D Biol Crystallogr **60:** 1167-1169

Kroymann J, Donnerhacke S, Schnabelrauch D, Mitchell-Olds T (2003) Evolutionary dynamics of an Arabidopsis insect resistance quantitative trait locus. Proc Natl Acad Sci USA **100:** 14587-14592

Kroymann J, Textor S, Tokuhisa JG, Falk KL, Bartram S, Gershenzon J, Mitchell-Olds T (2001) A gene controlling variation in Arabidopsis glucosinolate composition is part of the methionine chain elongation pathway. Plant Physiol **127:** 1077-1088

Lee CJ, Serif GS (1968) 2-Amino-6-(methylthio)caproic acid, a methionine homolog and precursor of progoitrin. Biochimica et Biophysica Acta **165:** 569-571

Lee CJ, Serif GS (1970) Precursor role of [14C, 15N]-2-amino-6-(methylthio)caproic acid in progoitrin biosynthesis. Biochemistry **9:** 2068-2071

Magrath R, Bano F, Morgner M, Parkin I, Sharpe A, Lister C, Dean C, Turner J, Lydiate D, Mithen R (1994) Genetics of aliphatic glucosinolates: I. Side chain elongation in Brassica napus and Arabidopsis thaliana. Heredity **72:** 290-299

Mikkelsen MD, Petersen BL, Glawischnig E, Jensen AB, Andreasson E, Halkier BA (2003) Modulation of CYP79 genes and glucosinolate profiles in Arabidopsis by defense signaling pathways. Plant Physiol **131:** 298-308

Nakamura K, Inoue K, Ushio K, Oka S, Ohno S (1988) Stereochemical control on yeast reduction of α-keto esters. Reduction by immobilized bakers' yeast in hexane. J Org Chem **53:** 2589-2593

Naur P, Petersen BL, Mikkelsen MD, Bak S, Rasmussen H, Olsen CE, Halkier BA (2003) CYP83A1 and CYP83B1, two nonredundant cytochrome P450 enzymes metabolizing oximes in the biosynthesis of glucosinolates in Arabidopsis. Plant Physiol **133:** 63-72

Piotrowski M, Schemenewitz A, Lopukhina A, Muller A, Janowitz T, Weiler EW, Oecking C (2004) Desulfoglucosinolate sulfotransferases from Arabidopsis thaliana catalyze the final step in the biosynthesis of the glucosinolate core structure. J Biol Chem **279:** 50717-50725

Reichelt M, Brown PD, Schneider B, Oldham NJ, Stauber EJ, Tokuhisa J, Kliebenstein DJ, Mitchell-Olds T, Gershenzon J (2002) Benzoic acid glucosinolate esters and other glucosinolates from Arabidopsis thaliana. Phytochemistry **59:** 663-671

Rogers SO, Bendich AJ (1985) Extraction of DNA from milligram amounts of fresh, herbarium and mummified plant tissues. Plant Mol Biol **5:** 69-76

Roxburgh CJ (1997) Protocol for purifying α-ketocarboxylic acids. Aldrichim Acta **30:** 74

Schreiber J (1956) D'une methode de preparation générale des acide α cétoniques aliphatique. B Soc Chim Fr Mémoires**:** 1361-1363

Schuster J, Knill T, Reichelt M, Gershenzon J, Binder S (2006) Branched-chain aminotransferase4 is part of the chain elongation pathway in the biosynthesis of methionine-derived glucosinolates in Arabidopsis. Plant Cell **18:** 2664-2679

Schwab W (2003) Metabolome diversity: too few genes, too many metabolites? Phytochemistry **62:** 837-849

Somers JM, Amzallag A, Middleton RB (1990) Use of T7 RNA polymerase to direct expression of cloned genes. Methods Enzymol **185:** 60-89

Studier FW, Rosenberg AH, Dunn JJ, Dubendorf JW (1990) Use of T7 RNA polymerase to direct expression of cloned genes. Methods Enzymol **185:** 60-89

Textor S, Bartram S, Kroymann J, Falk KL, Hick A, Pickett JA, Gershenzon J (2004) Biosynthesis of methionine-derived glucosinolates in Arabidopsis thaliana: Recombinant expression and characterization of methylthioalkylmalate synthase, the condensing enzyme of the chain elongation cycle. Planta **218:** 1026-1035

Tholl D, Chen F, Petri J, Gershenzon J, Pichersky E (2005) Two sesquiterpene synthases are responsible for the complex mixture of sesquiterpenes emitted from Arabidopsis flowers. Plant J **42:** 757-771

Tokuhisa J, de Kraker J-W, Textor S, Gershenzon J (2004) The biochemical and molecular origins of aliphatic glucosinolate diversity in Arabidopsis thaliana. *In* JT Romeo, ed, Secondary Metabolism in Model Systems, Recent Advances in Phytochemistry, Vol 38. Elsevier Science, Amsterdam, pp 19-38

Vogel AI, Furniss BS (1996) Vogel's textbook of practical organic chemistry. Longman Press, Harlow

Wan CY, Wilkins TA (1994) A modified hot borate method significantly enhances the yield of high-quality RNA from cotton (Gossypium hirsutum L.). Anal Biochem **223:** 7-12

Wilkinson GN (1961) Statistical estimations in enzyme kinetics. Biochem J **80:** 324-332

Wink M (2003) Evolution of secondary metabolites from an ecological and molecular phylogenetic perspective. Phytochemistry **64:** 3-19

Wittstock U, Halkier BA (2002) Glucosinolate research in the Arabidopsis era. Trends Plant Sci **7:** 263-270

Wittstock U, Kliebenstein DJ, Lambrix V, Reichelt M, Gershenzon J (2003) Glucosinolate hydrolysis and its impact on generalist and specialist insect herbivores. *In* JT Romeo, ed, Integrative Phytochemistry: from Ethnobotany to Molecular Ecology, Recent Advances in Phytochemistry, Vol 37. Elsevier Science, Amsterdam, pp 101-125

FIGURE LEGENDS

Figure 1. Scheme of methionine-derived glucosinolate biosynthesis in *A. thaliana*. This process can be divided into the methionine chain elongation cycle (I), and the biosynthesis of the core glucosinolate structure (II). The parent methylthioalkyl glucosinolates can undergo further side chain modifications.

Figure 2. Immunocytochemical localization of MAM3 protein in *A. thaliana* leaves.
Cross-section of leaves were probed with anti-MAM3 antibody (A, C) or with preimmune serum (E), followed by a fluorescence-labelled secondary antibody. A strong green fluorescence label within chloroplasts in (A) and (C) is indicative of the MAM3 protein. Chloroplasts are defined by positive DAPI-staining (B) of the same section as shown in (A) and by starch granules visualized in (D) by the differential interference contrast image of (C). Negative control performed by treatment with preimmune serum did not exhibit any label (E). Bars represent 20 µm in (A), (B), (E) and 5 µm in (C), (D), respectively.

Figure 3. Glucosinolate profile of leaves (A) and seeds (B) of *MAM3* mutants compared to Columbia-0 wild-type. Glucosinolates were purified as desulfoglucosinolates, fractionated by reverse-phase HPLC and individually identified and quantified. Individual methionine-derived glucosinolates are grouped according to their chain length (number of methylene carbons in the R group, C_2 through C_8), while indole glucosinolates are depicted separately. Data show the mean and standard error of three replicate samples.

Figure 4. Glucosinolate profile of leaves (A) and seeds (B) of the *MAM1* insertion mutant *gsm1-3* compared to Col-0 wild-type. Aliphatic glucosinolates sum up to 22.4/87.2 µmol * gDW^{-1} (leaf/seed) in wild type and 27.3/96.9 µmol * gDW^{-1} in the mutant. Glucosinolates were isolated, identified and quantified as explained in the Fig. 3 legend.

Figure 5. Steady state mRNA transcript levels of *MAM1* and *MAM3* in tissues of Col-0 wild-type and *MAM3* mutant lines determined by reverse-transcriptase PCR. DNA fragments for individual transcripts of ACT8 (actin), MAM1 and MAM3 were generated by PCR amplification of products from reverse transcriptase activity primed by oligo-dT hybridization to the RNA. The PCR products are shown after separation on 1% agarose gels stained with

ethidium bromide. Tissue source: 1- roots, 2- mature leaves, 3- expanding leaves, 4- flowers, 5- siliques.

Table 1. Nomenclature for *A. thaliana* (Columbia) Genes of the Isopropylmalate Synthase / MAM Synthase Gene Family Used in Recent Publications.

AGI Locus Code	N-terminal Sequence	BACs	Kroymann et al., 2001	Junk and Mourad, 2002	Field et al., 2004	This Paper
At1g18500	MASSLLR	F15H18	-	EST116C2 T7	*MAML-4*	*IPMS1*
At1g74040	MESSILK	F2P9.9	-	*IMS1*	*MAML-3*	*IPMS2*
At5g23010	MASSLLT	CT20O7	*MAM1*	*IMS3*	*MAM1/L*	*MAM1*
-[a]	MASSLLT[b]	-	-	-	-	*MAM2*
At5g23020	MASLLLT	MYJ24	*MAM-L*	*IMS2*	*MAM1/L*	*MAM3*

[a] Col-0 ecotype lacks *MAM2*. The gene would be located between At5g23000 and At5g23010 (*MAM1*) on the Col genome (Kroymann et al., 2003).

[b] *Landsberg erecta* (Ler-0)

Table 2. Suitability of 2-Oxo Acids as Substrates For MAM3-Mediated Condensation with Acetyl-CoA

2-Oxo Acid Substrate	Structure	Resulting glucosinolate	Suitability[a]
4-Methylthio-2-oxobutanoate	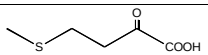	C_3	+
2-Oxo-hexanoate	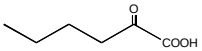	C_3	+
5-Methylthio-2-oxopentanoate	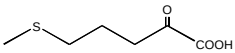	C_4	+
2-Oxo-heptanoate	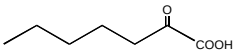	C_4	+
6-Methylthio-2-oxohexanoate	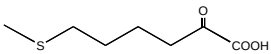	C_5	+
2-Oxo-octanoate	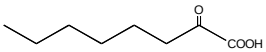	C_5	+
2-Oxo-nonanoate	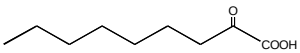	C_6	+
8-Methylthio-2-oxooctanoate	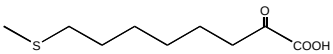	C_7	+
2-Oxo-decanoate	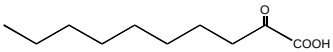	C_7	+
9-Methylthio-2-oxononanoate	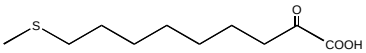	C_8	+
2-Oxo-undecanoate	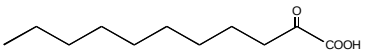	C_8	+
2-Oxo-dodecanoate	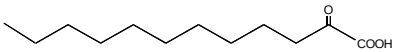	C_9	-

[a] +, condensation product formed; -, condensation product not formed

Table 3. Kinetic Parameters for Various 2-Oxo Acids with Recombinant MAM3[a].

Substrate	K_m [μM]	V_{max} [nmol $min^{-1}mg^{-1}$]	k_{cat} [s^{-1}]	k_{cat}/K_m [$M^{-1}s^{-1}$]
4-Methylthio-2-oxobutanoic acid (→C_3 glucosinolates)	932 ± 56	1448 ± 299	1.3 ± 0.3	1380
5-Methylthio-2-oxopentanoic acid (→C_4 glucosinolates)	476 ± 199	1495 ± 679	1.3 ± 0.6	2730
6-Methylthio-2-oxohexanoic acid (→C_5 glucosinolates)	463 ± 210	2869 ± 768	2.5 ± 0.7	5400
8-Methylthio-2-oxooctanoic acid (→C_7 glucosinolates)	253 ± 123	364 ± 143	0.3 ± 0.1	1280
9-Methylthio-2-oxononanoic acid (→C_8 glucosinolates)	81 ± 21	31 ± 8	0.03 ± 0.01	370
2-Oxoisovalerate	1000 ± 200	199 ± 38	0.18 ± 0.03	200
Pyruvate	8600 ± 4300	191 ± 48	0.17 ± 0.04	23
Acetyl-CoA	2300 ± 1200	3344 ± 1428	3.0 ± 1.3	1300

[a]Data presented are means ± standard deviations of at least 5 replicates per substrate

Table 4. Glucosinolate Content (µmol * gDW^{-1}) in Leaves of *gsm2-1* and Lines Transformed With 35S::*MAM3*[a]

	C_3	C_4	C_5	C_6	C_7	C_8	ΣCi
Col-0 wild type	2.7	16.3	0.5	0.3	0.4	2.2	22.4
gsm2-1	2.5	18.2	0.6	0.2	n.d.	n.d.	21.5
T_2 Line 1	2.3	6.5	n.d.	1.0	3.2	8.6	21.6
T_2 Line 2	3.9	8.0	n.d.	1.6	6.2	15.9	35.5
T_2 Line 3	4.1	6.4	n.d.	1.1	3.9	10.1	25.7

[a]Presented are analyses of Col-0 wild-type, the *gsm2-1* parent line and three lines randomly selected from a T_2 segregating population that had detectable levels of the introduced *MAM3* transcript. n.d., not detected.

Figure 1

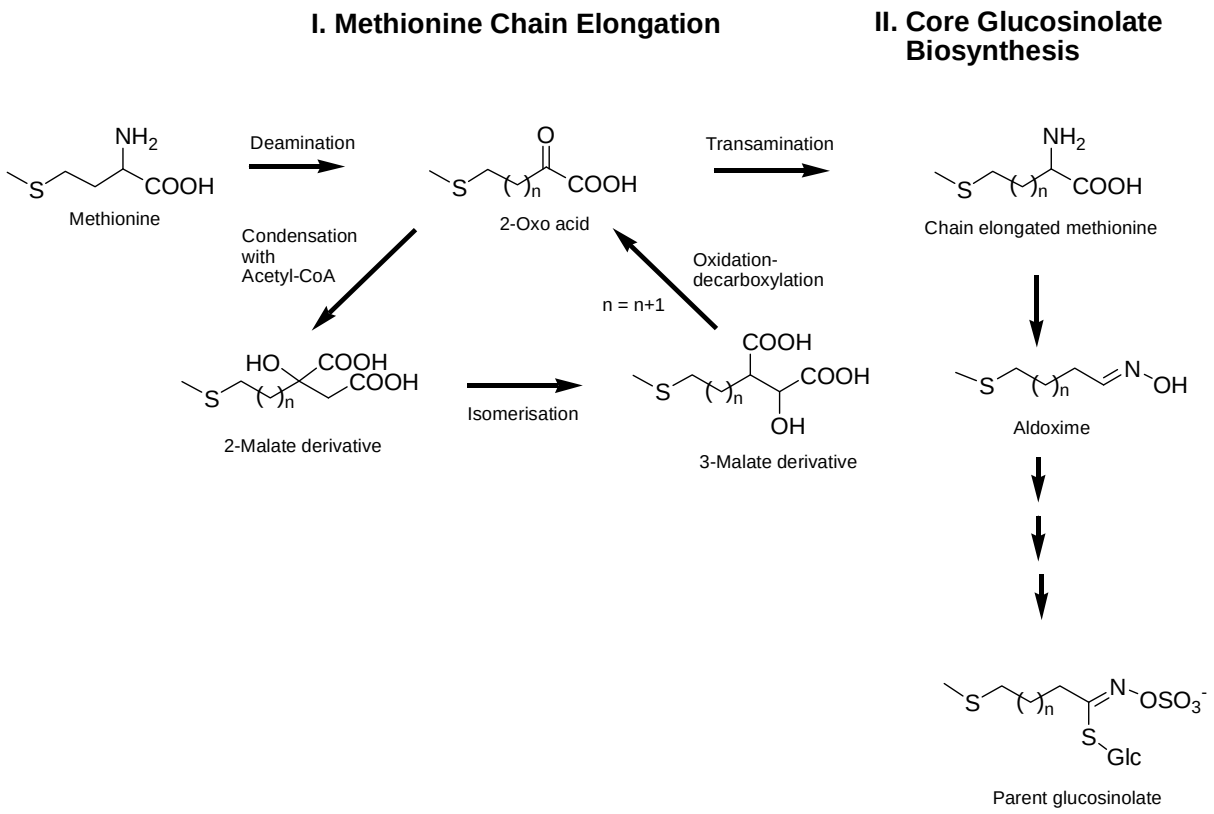

Figure 2

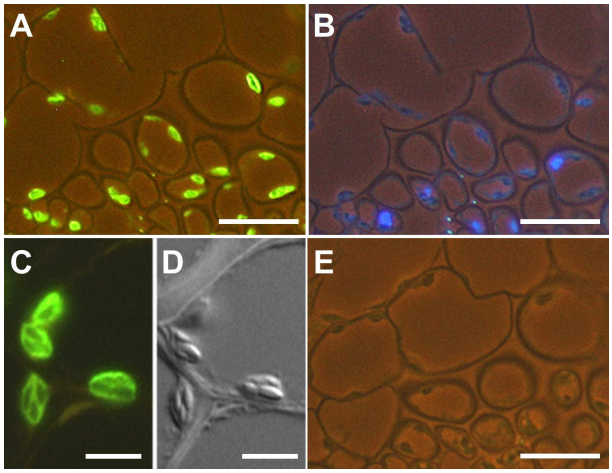

Figure 3

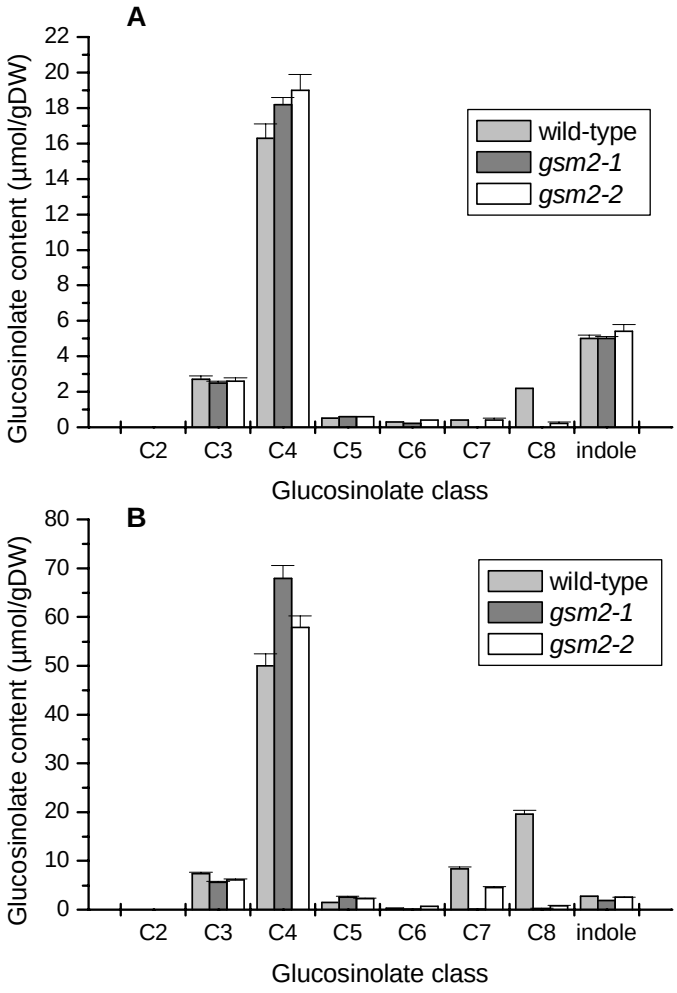

Figure 4

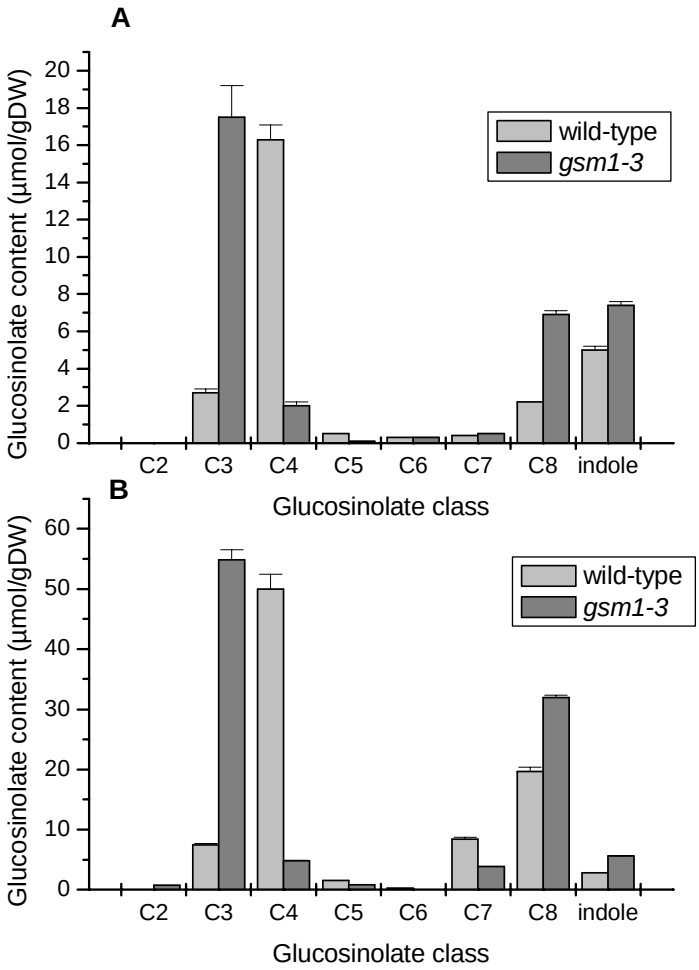

Figure 5